THE JOURNAL OF PHYSICAL CHEMISTRY B

ARTICLE

pubs.acs.org/JPCB

Correlations for Adsorption of Oxygenates onto Zeolites from Aqueous Solutions

Elizabeth E. Mallon,[†] Ian J. Babineau,[†] Joshua I. Kranz,[†] Yasmine Guefrachi,[§] J. Ilja Siepmann,[‡] Aditya Bhan,[*,†] and Michael Tsapatsis[*,†]

[†]Department of Chemical Engineering and Materials Science and [‡]Department of Chemistry, University of Minnesota, Minneapolis, Minnesota 55455, United States

[§]Department of Chemical Engineering, The Petroleum Institute, Abu Dhabi, United Arab Emirates

Supporting Information

ABSTRACT: Henry's constants (K_{ads}) for adsorption of C_3 polyfunctional molecules onto zeolites from aqueous solutions at 278 K were obtained and compared with the octanol−water partition coefficients, K_{ow}, which were calculated using the prevalent ClogP group contribution method. K_{ads} increases linearly with K_{ow} for these adsorbates on H−ZSM-5 (MFI), FAU, BEA, and ITQ-1 (MWW). K_{ads} values for C_2−C_6 diol adsorption at 278 K are also linearly correlated with K_{ow} regardless of interactions in the bulk phase as measured by the solution activity coefficient. Exceptions to the correlation established between K_{ads} and K_{ow} are the adsorption of 1,2,ω-triols with carbon number greater than three on H−ZSM-5 and adsorption of all oxygenates studied on FER, which we postulate to be due to the effect of changing adsorption configuration with adsorbate/zeolite structure which cannot be captured by K_{ow} alone. These results enable the prediction of separation selectivities of biomass-derived compounds on zeolite adsorbents.

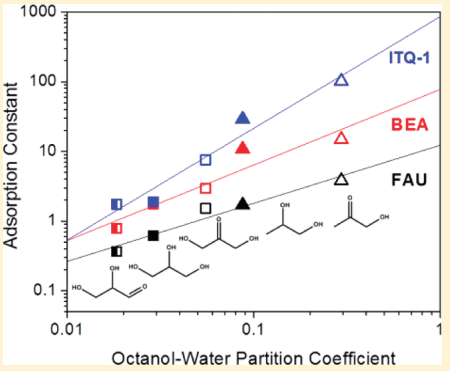

INTRODUCTION

The ability of zeolites to discriminate between alkanes of differing carbon number and degree of branching has led to their prevalent use as cracking, isomerization, and alkylation catalysts and in turn inspired fundamental research on the interactions between zeolites and alkanes. It has been shown using calorimetric, gravimetric, spectroscopic, and computational studies that the enthalpy of adsorption of linear and branched alkanes increases with carbon number on several zeolite frameworks including MFI,[1−4] MOR,[3−5] FAU,[2,3,5,6] FER,[6,7] TON,[6] MTW,[6] UTD-1,[6] MWW,[8] and BEA,[4] which is due to an increase in dispersion interactions between the adsorbate and zeolite pore walls with increasing carbon number. The conclusion that confinement of the adsorbate in the zeolite pores is a significant contributor to the energy of adsorption is also supported by the observation in a calorimetric study that the enthalpy of adsorption of linear and branched alkanes decreases with an increase in zeolite pore size when comparing the MFI, MOR, and FAU frameworks.[3]

The effect of chemical composition on alkane adsorption has also been explored. Eder et al. obtained the enthalpy and Henry's constants for adsorption of C_3−C_9 linear alkanes on pure silica and aluminum-containing samples of the MFI and FAU frameworks using calorimetry.[2,3] The authors noted that the materials with aluminum incorporated in the framework, which gives rise to Brønsted acid sites, exhibited 10 and 6 kJ mol^{-1} increases in the adsorption enthalpy on the MFI and FAU frameworks, respectively, for all alkanes studied when compared with the siliceous materials. The contribution of acid site interactions to the energy of adsorption was low; it ranged from ∼10 to 20% of the total enthalpy measured for C_3−C_9 linear alkanes on H−MFI. This increase in adsorption enthalpy was compensated by a commensurate increase in adsorption entropy, and therefore a comparable free energy of adsorption at ambient temperatures was obtained on materials with the same framework irrespective of the number of acid sites. Overall, these studies show that the chemical composition of the zeolite framework has an effect on the enthalpy and entropy of adsorption for saturated hydrocarbons, but the energy of adsorption is primarily affected by the dispersion interactions between the adsorbate and zeolite pore walls.

Several authors have probed the primary interactions for adsorption of alcohols, which contain the additional functionality of a polar −OH group when compared with alkanes, on zeolites. Multiple studies have noted using gravimetry combined with calorimetric[9] and spectroscopic[10,11] approaches that alcohols preferentially adsorb via hydrogen bonding of the −OH group with the zeolite Brønsted acid sites. Although this results in an enthalpy of adsorption 50−60 kJ mol^{-1} greater for coverages less than 400 μmol g^{-1} when comparing siliceous and aluminum-containing MFI zeolites, the free energy of adsorption is relatively

Received: August 23, 2011
Published: September 14, 2011

Table 1. Structures and Chemical Compositions of Adsorbents

zeolite name	framework	Si/Al	Al/uc
CP914	FER	29[a]	1.2
ITQ-1	MWW	∞	0
CBV28014 (H−ZSM-5)	MFI	140	0.7
CP811C-300	BEA	100	0.6
CBV760	FAU	30	6.2

[a] Si/Al determined using inductively coupled plasma optical emission spectroscopy by Galbraith. All other Si/Al values from vendor or approximated from synthesis procedure.

similar due to compensation from the entropy of adsorption.[9] This result, in conjunction with the finding that the heat of adsorption of alcohols increases 15−20 kJ mol^{-1} with each additional carbon,[9] highlights that dispersion forces which arise from interaction between the adsorbate and the zeolite pore walls are also a crucial factor in the adsorption affinity of alcohols.

Recently, we identified that many of the trends observed for the vapor phase adsorption of alkanes and alcohols on zeolites are also found for the adsorption of polyols, hydrocarbons functionalized with multiple −OH groups, onto zeolites from aqueous solutions. Specifically, we found that K_{ads} for these systems increases exponentially with carbon number on the MFI, BEA, and MWW frameworks,[12] which is in accordance with observations made for the adsorption of alkanes, olefins, and epoxides onto TS-1 from a variety of solvents.[13,14] When this result was considered along with the observation that K_{ads} for propylene glycol adsorption on the FAU, MOR, BEA, MFI, and MWW materials increases with a decrease in zeolite pore size, it was concluded that dispersion forces between the adsorbate and the zeolite pore wall are a primary driving force for polyol adsorption.

For MFI materials it was found that changing the Si/Al ratio from 10 to ∞ resulted in a maximum increase in K_{ads} of 50%; a similar indifference to MFI chemical composition was noted by Ramachandran et al. for the adsorption of hexene onto MFI from methanol.[15] When compared with the order of magnitude increase in K_{ads} with a decrease in zeolite pore size (compare FAU with MWW), it was concluded that dispersion interactions between the adsorbate and the zeolite pore wall are dominant compared to electrostatic interactions for polyol adsorption. Another outcome of our study was identification that the affinity for polyol adsorption from aqueous solutions decreases an order of magnitude with the addition of an −OH group.[12] However, the origin of such a marked effect of C/OH ratio, as well as the effects of changing oxygen functionality and solution phase thermodynamics, on zeolite adsorption affinity remained unclear at the time of our earlier report.

Here, we show on the basis of a linear correlation between K_{ads} and the octanol−water partition coefficient, K_{ow}, that the effects of C/OH ratio and chemical functionality on oxygenate adsorption are the result of both interactions in the solution phase and strong dispersion interactions in the zeolite. This novel correlation enables the facile and accurate prediction of K_{ads} for polyfunctional C_2−C_6 molecules on zeolites varying in pore size and connectivity. Also presented are data for some adsorbate−zeolite systems that do not obey this correlation, demonstrating that size exclusion can play a critical role in oxygenate adsorption which allows for enhanced separation of molecules with similar K_{ow} values. We also show that solution nonidealities do not significantly perturb the correlation for C_2−C_4 diols on H−ZSM-5, indicating that the relationship between K_{ads} and K_{ow} is a strong function of dispersion forces in the lipophilic octanol/zeolite phase.

METHODS

Adsorption Experiments. All experiments were completed using the protonated form of the FER, MFI, BEA, MWW, and FAU frameworks which had Si/Al ratios ranging from 29 to ∞ (6.2 to 0 Al/unit cell) as shown in Table 1. Sources for procured materials, methods for synthesized materials, and the pretreatment conditions have been reported elsewhere.[12] X-ray diffraction was used to verify the structures of all zeolites.

All adsorbates were C_2−C_6 hydrocarbons with two to three oxygen functional groups. The adsorbates hydroxyacetone (Sigma Aldrich, 90%), propylene glycol (Fischer Scientific, >99%), and glycerol (Sigma-Aldrich, >99.5%) were in the liquid phase at ambient temperature and atmospheric pressure. Dihydroxyacetone (Acros Organics USA, >98.5%, dimer) and glyceraldehyde (Sigma Aldrich, >90%, dimer) were in the solid phase at ambient temperature and atmospheric pressure. Sources and purities of the other oxygenate adsorbates can be found in ref 12. Dihydroxyacetone stock solutions were prepared 24 h in advance of the start of the experiment to allow dimers to dissociate into monomers at ambient temperature, as confirmed by ^{13}C NMR analysis.[16,17]

Aqueous solutions with a volume of 1 mL were prepared in closed glass vials. Zeolite samples were added to each solution in the amount of 100 ± 5 mg after the solutions had been chilled for 1 h at 278 ± 0.5 K. The slurries were stirred at 600 rpm for approximately 24 h while maintaining a temperature of 278 ± 0.5 K. The slurries were then filtered using a 3 mL Monoject syringe fitted with a 0.2 μm GHP (polypropylene) syringe filter to remove the zeolite particles, and the filtrates were prepared for analysis with liquid chromatography.

The filtrate concentrations were analyzed using an Agilent 1200 high performance liquid chromatography (HPLC) system equipped with a refractive index detector (RID) and an autosampler. The autosampler removed 75 μL of sample from a single vial and injected the contents into a stream of 0.005 M sulfuric acid (H_2SO_4) in deionized water with a flow rate of 0.008 cm^3 s^{-1}. The stream passed through a Bio-Rad Aminex HPX-87H polystyrene packed column heated to 333 K, and the column pressure was maintained at 40−60 bar. The outlet stream passed through the RID, which was heated to 323 K. The RID signal output was recorded and plotted against time, and the adsorbate peak was identified from the retention time. No reaction products that would indicate chemisorption of the adsorbates on the zeolites were identified. The relative signal intensities of the adsorbate and a glycerol or propylene glycol internal standard were used to determine the final concentration of each solution. The difference in the initial and final concentrations and the total volume of the solution were used to calculate the amount of compound adsorbed onto the zeolite.

Computation of Octanol−Water Partition Coefficients (K_{ow}). Multiple methods were tested for their accuracy in computing the experimental K_{ow} values (obtained from the SRC PhysProp[18] or Sangster Research Laboratories LOGKOW[19] databases) for 22 C_1−C_6 polyols, aldehydes, ketones, and ethers which have functionality representative of the adsorbates used in this study as shown in the Supporting Information (Table S1).

Table 2. Sources of log *P* Computational Methods and Comparison of Results for the Test Set of Experimental Values from the SRS PhysProp Database

model	software	access	rmse[a]
ClogP[40]	ClogP 4.0	ChemBioDraw Ultra 11.0	0.114
AlogP[41]	DragonX	www.vcclab.org	0.236
LogKow[42]	KowWin 1.67	www.chemspider.com	0.175
ACD/LogP[43]	ACD/LogP	www.chemspider.com	0.189
XlogP3[20]	XlogP3 3.3.2	www.vcclab.org	0.118
MlogP[44]	DragonX	www.vcclab.org	0.297
ALOGPS[45,46]	ALOGPS 2.1	www.vcclab.org	0.203

[a] Root-mean-square-error between experimental and predicted values.

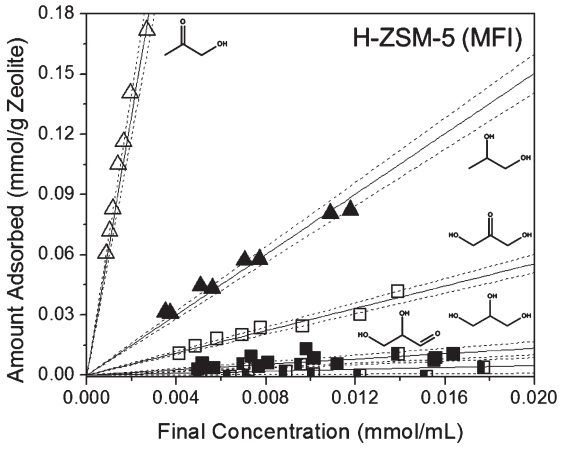

Figure 1. Adsorption isotherms at 278 K for hydroxyacetone (△), propylene glycol (▲), dihydroxyacetone (□), glycerol (■), and glyceraldehyde (◧) on H−ZSM-5. Solid lines represent least-squares linear regressions. Dashed lines represent 95% confidence intervals.

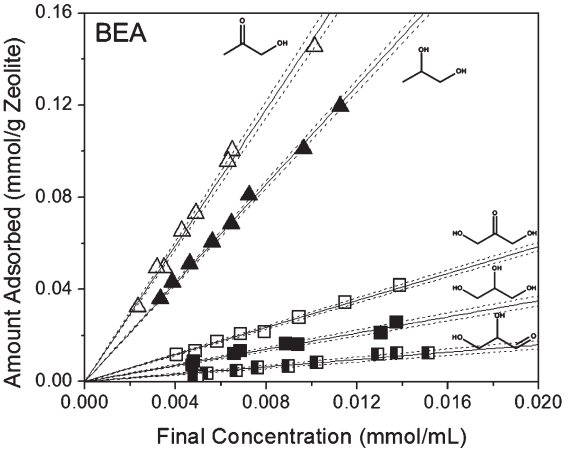

Figure 2. Adsorption isotherms at 278 K for hydroxyacetone (△), propylene glycol (▲), dihydroxyacetone (□), glycerol (■), and glyceraldehyde (◧) on BEA. Solid lines represent least-squares linear regressions. Dashed lines represent 95% confidence intervals.

All computational methods explored and the root-mean-square errors (RMSE) between the computed and experimental PhysProp values for the test set of molecules are shown in Table 2. The ClogP method achieved the lowest rmse regardless of the experimental

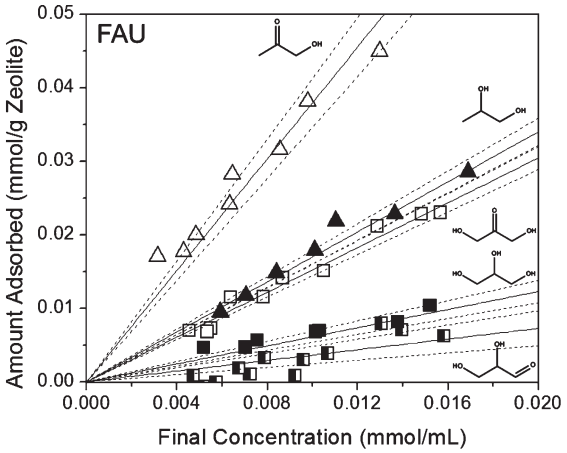

Figure 3. Adsorption isotherms at 278 K for hydroxyacetone (△), propylene glycol (▲), dihydroxyacetone (□), glycerol (■), and glyceraldehyde (◧) on FAU. Solid lines represent least-squares linear regressions. Dashed lines represent 95% confidence intervals.

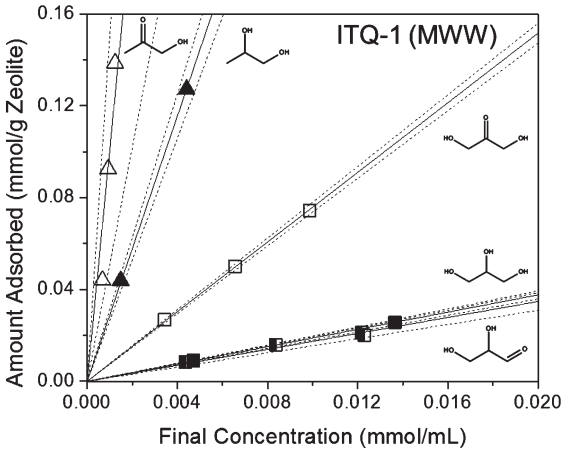

Figure 4. Adsorption isotherms at 278 K for hydroxyacetone (△), propylene glycol (▲), dihydroxyacetone (□), glycerol (■), and glyceraldehyde (◧) on ITQ-1. Solid lines represent least-squares linear regressions. Dashed lines represent 95% confidence intervals.

database used and was therefore chosen for calculation of the K_{ow} values for the C_3 adsorbates used in this study. This approach is supported by the observation that the ClogP algorithm produces the lowest rmse for molecules with less than 20 heavy atoms when compared with other widely available methods.[20,21]

■ RESULTS AND DISCUSSION

Effect of Adsorbate Functionality. Adsorption isotherms for the C_3 polyfunctional adsorbates on the H−ZSM-5 (MFI), BEA, FAU, and ITQ-1 (MWW) materials are shown in Figures 1, 2, 3, and 4, respectively. On these four frameworks, the affinity for adsorption at low concentrations increases in the order glyceraldehyde < glycerol < dihydroxyacetone < propylene glycol < hydroxyacetone, which indicates that the affinity for adsorption is dependent on the oxygen functional groups since all adsorbates of interest contain three carbons each. The order of magnitude decrease in adsorption with increasing −OH number

Table 3. K_{ow} Values for the Adsorbates

adsorbate	molecular formula	K_{ow}[a]
hydroxyacetone[b]	CH_3COCH_2OH	0.294
propylene glycol[c]	$CH_3CH(OH)CH_2OH$	0.087
dihydroxyacetone[b]	$HOCH_2COCH_2OH$	0.055
glycerol[c]	$HOCH_2CH(OH)CH_2OH$	0.029
glyceraldehyde[b]	$HOCH_2CH(OH)CHO$	0.018
1,2-hexanediol[c]	$CH_3(CH_2)_3CH(OH)CH_2OH$	3.364
1,2-butanediol[c]	$CH_3CH_2CH(OH)CH_2OH$	0.294
1,3-propanediol[c]	$HO(CH_2)_3OH$	0.092
ethylene glycol[c]	$HO(CH_2)_2OH$	0.043
1,2,6-hexanetriol[c]	$HO(CH_2)_4CH(OH)CH_2OH$	0.035
1,2,4-butanetriol[c]	$HO(CH_2)_2CH(OH)CH_2OH$	0.014

[a] Calculated using the ClogP[40] group contribution method. [b] Adsorbate in this study. [c] Adsorbate in this study and Mallon et al.[12]

(compare glycerol with propylene glycol and dihydroxyacetone with hydroxyacetone) has been observed previously on the MFI framework,[12] and from these data it is noted that the trend is consistent on BEA, FAU, and ITQ-1. Exchanging an −OH group with a =O also has a significant effect on adsorption affinity; the exchange of −OH for =O on a primary carbon (compare glycerol and glyceraldehyde) decreases adsorption 10−90% whereas the exchange at a secondary carbon *increases* adsorption 200−400% as evidenced by comparing glycerol/dihydroxyacetone and propylene glycol/hydroxyacetone on H−ZSM-5, BEA, FAU, and ITQ-1.

It was of interest to compare the adsorption isotherm results with the octanol−water partition coefficient, K_{ow}, for the adsorbates since this is a well-established method for assessing the hydrophilicity or lipophilicity of organic molecules. The K_{ow} values calculated with the ClogP group contribution method for the C_3 oxygenate adsorbates in this study are shown in Table 3. Inspection of these values reveals that they increase in the order glyceraldehyde < glycerol < dihydroxyacetone < propylene glycol < hydroxyacetone, which is the same as the rank for adsorption strength observed on H−ZSM-5, BEA, FAU, and ITQ-1, indicating that K_{ow} can be used to predict relative adsorption affinities of oxygenates onto zeolites.

Correlating K_{ads} for Polyfunctional Adsorbates. In order to better compare K_{ow} with the adsorption results, K_{ads} values were extracted from the adsorption isotherms. Using gravimetric methods, it has been shown that water adsorption on zeolites only occurs at the Brønsted acid sites that arise from incorporation of aluminum into the zeolite framework[22−24] and silanol groups at the external crystal surface and defects;[9,25] it has also been observed with gravimetric, calorimetric, and FTIR spectroscopy methods that water adsorbs with a heat of adsorption ~30 kJ mol^{-1} less than methanol,[9] and during competitive adsorption methanol will displace water physisorbed on Brønsted acid sites.[10] Although water may not be competing for adsorption sites, it is important to note that water is possibly hydrogen bound to the adsorbed oxygenates as demonstrated by Krishna and van Baten using CBMC simulations.[26] This interaction would have an effect on the energetics of adsorption and therefore on K_{ads}; however, we cannot discern the magnitude of these effects and have therefore adopted an initial approach where we have neglected adsorbate−water interactions within the zeolite pores and are

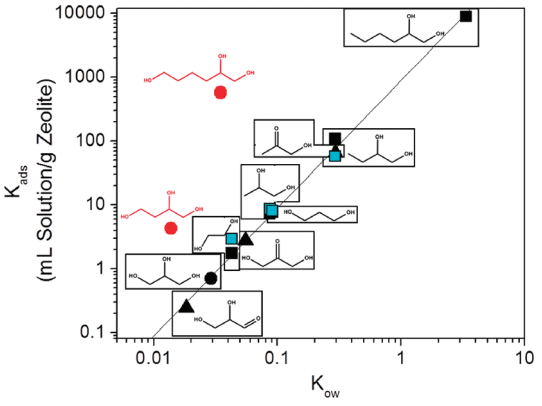

Figure 5. Measured K_{ads} versus K_{ow} on MFI CBV28014 at 278 K for carbonyl-containing molecules (▲), diols (■), and 1,2,ω-triols (● and red solid circles). The solid line represents the least-squares linear regression on the black data points. Diol $K_{ads,intrinsic}$ values (cyan solid squares) obtained by decoupling the solution activity coefficients from the measured water−zeolite partition coefficients.

treating the adsorption isotherms here as single-component adsorption isotherms.

The data here are for coverages between ~0.001 and 1 oxygenate per unit cell, which represents less than 10% of the total micropore volume and is well below the maximum site occupancy and the regime where site heterogeneity or oxygenate−oxygenate interactions are expected to have an effect on adsorption based upon computational studies on the siting of straight and branched alkanes in MFI.[27,28] At these low coverages it is expected that the molecules preferentially adsorb in one type of adsorption site and adsorption is linearly correlated with concentration. Therefore, the data were fit using least-squares linear regression and the K_{ads} values were determined from the slope of the line.

Plotting K_{ads} versus K_{ow} for adsorption on H−ZSM-5 at 278 K reveals a linear correlation between affinity for adsorption and hydrophilicity/lipophilicity, as shown in Figure 5. K_{ads} values for C_2−C_6 diols on H−ZSM-5 at 278 K (isotherms presented in the Supporting Information, Figure S1) also fall on this linear correlation between K_{ads} and K_{ow}. It is clear that K_{ow}, which can be readily calculated using available software, is an accurate predictor of the adsorption affinity of polyfunctional oxygenates onto H−ZSM-5 from aqueous solutions with K_{ads} values spanning at least 5 orders of magnitude; this is the first demonstration of the predictive nature of K_{ow} for K_{ads} on zeolites from aqueous solutions.

Effect of Solution Thermodynamics. Although the linear correlation between K_{ads} and K_{ow} is practically useful, the interactions responsible for the trend are unknown. That is, hydrophobic interactions in water or dispersion forces in the lipophilic octanol/zeolite phase could both be used to explain the observed linear correlation between K_{ads} and K_{ow} for the diols, hydroxyketones, and glyceraldehyde. Thermodynamic definitions of chemical potential and equilibrium can be used to decouple the interactions, that is

$$\mu_{ads} = \mu_{bulk}$$

where μ_{ads} and μ_{bulk} are the chemical potentials of the adsorbate in the adsorbed and bulk phases, respectively. For a system of M identical adsorption sites, N adsorbate molecules with $N < M$,

and negligible adsorbate−adsorbate interactions, one can use statistical mechanics to derive the expression

$$\mu_{ads} = kT \ln\left[\frac{\theta}{(1-\theta)f}\right]$$

where $\theta = N/M$, k is the Boltzmann constant, and f is the partition function associated with a single adsorbed molecule.[29] Furthermore, if one considers equilibrium between the adsorbed phase and an ideal gas phase, one obtains

$$\theta = \frac{bp}{1 + bp}$$

where $b(T) = f(T)e^{\mu^\circ/kT}$ is an equilibrium constant and p is the pressure. This is a form of the Langmuir isotherm model. We use the same approach, but for equilibrium between the adsorbed phase and a solution phase, that is

$$kT \ln\left[\frac{\theta}{(1-\theta)f}\right] = \mu^\circ(T) + kT \ln a_i'$$

where a_i' is the activity of component i in solution and is defined as the product between the pure species fugacity (f_i'), mole fraction (x_i), and activity coefficient (γ_i) normalized to a reference fugacity (f_i°). This expression simplifies to

$$kT \ln\left[\frac{\theta}{(1-\theta)f}\right] = \mu^*(T) + kT \ln x_i\gamma_i$$

where $\mu^*(T)$ is the chemical potential of the pure liquid species. Following the same procedure as for the Langmuir isotherm, one obtains

$$\theta = \frac{b\gamma_i x_i}{1 + b\gamma_i x_i}$$

where $b(T) = f(T)e^{\mu^*/kT}$ is now defined as the equilibrium constant.

At low concentrations where $1 \gg b\gamma_i x$, we find that $\theta = b\gamma_i x_i$ or that the coverage, θ, is directly proportional to the solution mole fraction, x_i, with a slope equal to $b\gamma_i$. This equation has the same form as Henry's law, which we have applied to the isotherms presented here. Therefore, the proportionality constant in our experiments, K_{ads}, for the linear relationship between the amount adsorbed and the final solution concentration, is not the intrinsic K_{ads} value for adsorption from an ideal gas phase. Rather, this value is a combination of interactions in the solution phase and the adsorbed phase, that is, $K_{ads,measured} = \gamma_i K_{ads,intrinsic}$.

Now that it has been shown that $K_{ads,measured}$ is the result of the product between the solution activity coefficient and $K_{ads,intrinsic}$ value, it follows that if the activity coefficient is known then $K_{ads,intrinsic}$ can be determined. Since the concentrations used for this and our previous study[12] range from 1 to 25 μmol cm^{-3}, which is below the concentration used by Suleiman and Eckert[30] to obtain infinite dilution activity coefficients using a dew point technique, we considered infinite dilution activity coefficients, which are essentially a measure of interactions between a single solute molecule surrounded by solvent, as appropriate for decoupling $K_{ads,measured}$ and $K_{ads,intrinsic}$. The $K_{ads,intrinsic}$ values obtained are also plotted in Figure 5, and it can be deduced from this analysis that increasing diol carbon number decreases water solubility which has an effect on $K_{ads,measured}$, but the systematic increase in $K_{ads,measured}$ with diol carbon number can be attributed to increased dispersion interactions. This result for diol adsorption is consistent with the well-documented literature on single component alkane adsorption on the MFI framework, where it has been shown that K_{ads} increases exponentially with carbon number.[2,4] Furthermore, it has been shown using density functional calculations that the increasing stability of both physisorbed and chemisorbed C_1-C_4 alcohols on H−ZSM-5 with increasing carbon number is due to dispersive van der Waals interactions consistent with our hypothesis that the increase in K_{ads} with increasing 1,2-diol carbon number is due to confinement in the zeolite pore.[31]

When the infinite dilution coefficients at 298 K for 1-propanol[32] (13.8) and 1,2-propanediol (1.0) are compared, it can be deduced that the addition of an −OH group decreases the activity coefficient by an order of magnitude. This trend also holds when 1-butanol[32] (55.2) is compared with 1,2-butanediol (2.0).[12] Therefore, interactions between water and the adsorbate in the bulk as measured by the activity coefficient may be responsible for the inversely proportional relationship between K_{ads} and −OH number.

Effect of Zeolite Structure. The zeolite topology can also play a significant role in the adsorption of oxygenates. For example, it can be noted from Figure 5 that the K_{ads} values for 1,2,4-butanetriol and 1,2,6-hexanetriol are higher than what is expected from their K_{ow} values; this implies that K_{ads} is not a function of hydrophilicity/lipophilicity alone and K_{ow} does not adequately capture a critical component of 1,2,4-butanetriol and 1,2,6-hexanetriol adsorption on H−ZSM-5. Although errors in K_{ow} estimation may be partially responsible for this deviation (the XlogP3 method[19] yields K_{ow} values for these two compounds that are larger by factors of 3 and 6, respectively, see Table S2 in the Supporting Information), it could also arise due to differences in the adsorption environments of H−ZSM-5 and octanol. While adsorption in both phases is primarily driven by dispersion forces,[12,33] the strengths of these nonpolar interactions are significantly different as shown in Figure 5; the addition of a single methyl group leads to an increase in K_{ads} by an order of magnitude whereas K_{ow} only increases approximately 5-fold. This disparity in adsorption environment may be even more pronounced for 1,2,4-butanetriol and 1,2,6-hexanetriol than for glycerol, the only triol that falls on the correlation, due to preferential siting in H−ZSM-5. It has been shown via Monte Carlo simulations that isoalkanes with a carbon number less than 6 will completely reside within the channel intersection whereas the longer (C_7-C_{10}) alkanes adsorb with the bulky branched segment in the channel intersection and the slender hydrocarbon tail in the straight channel.[28,34] Therefore, we postulate that the long hydrocarbon chains of 1,2,4-butanetriol and 1,2,6-hexanetriol can reach into the straight channel where they have closer interaction with the pore walls resulting in the observed higher K_{ads} value than what is predicted by the correlation with K_{ow}. Exploration of the water−adsorbate and zeolite−adsorbate interactions using computational methods would best elucidate the cause of K_{ads} dependence on −OH number.

As shown in Figure 6, the linear increase in K_{ads} with increasing K_{ow} for the C_3 polyfunctional adsorbates in this study is observed not only on H−ZSM-5 but also on FAU, BEA, and ITQ-1 (MWW framework). It should also be noted that K_{ads} for each adsorbate increases as the smallest accessible pore size decreases from 6 (FAU) to 4 Å (ITQ-1). This effect is also evidenced by the increase in the correlation slope with decreasing pore size as shown in the top inset of Figure 6, a trend which can be utilized to

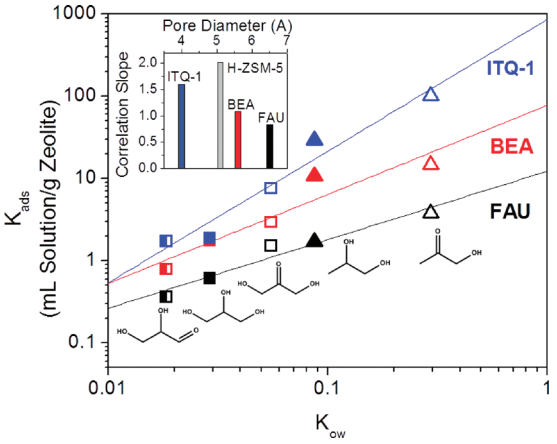

Figure 6. Measured K_{ads} versus K_{ow} for the carbonyl-containing adsorbates and their polyol counterparts on FAU, BEA, and ITQ-1 at 278 K. Solid lines represent least-squares linear regressions. (top inset) $K_{ads}-K_{ow}$ correlation slopes versus pore size for FAU, BEA, H−ZSM-5, and ITQ-1.

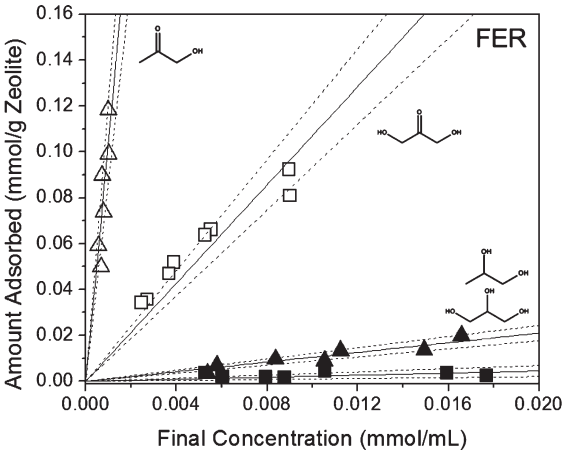

Figure 7. Adsorption isotherms at 278 K for hydroxyacetone (△), propylene glycol (▲), dihydroxyacetone (□), and glycerol (■) on FER. Glyceraldehyde adsorption was negligible. Solid lines represent least-squares linear regressions. Dashed lines represent 95% confidence intervals.

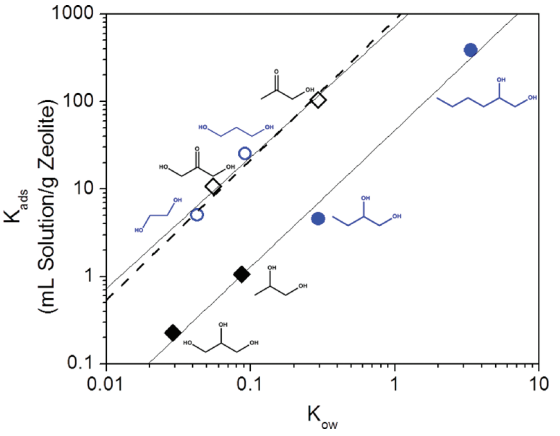

Figure 8. Measured K_{ads} versus K_{ow} for carbonyl-containing adsorbates (◇), their polyol counterparts (◆), and other 1,2- (blue solid circles) and 1,ω-diols (blue open circles) on FER at 278 K. Solid lines represent least-squares linear regressions. Dashed line represents the correlation found on ITQ-1.

adjust the correlation to predict adsorption on zeolites with a variety of pore sizes. The observed increase in adsorption affinity with decreasing zeolite pore size is not surprising; this result is in agreement with what has been found for C_1-C_6 alkane[6,7] and propylene glycol[12] adsorption which supports the conclusion that adsorption of polyfunctional molecules from aqueous solutions is a strong function of dispersion forces between the adsorbate and the zeolite pore walls.

After noting the versatility of K_{ow} as a predictor for K_{ads} of polyfunctional molecules in water over medium- and large-pore zeolites, it was of interest to employ a smaller, eight member-ring (MR) zeolite adsorbent to determine if shape selectivity effects could be used to disrupt this correlation and lead to large K_{ads} differences which may be desirable for highly selective separation processes. An analogous situation with hydrocarbons is the use of ITQ-12 (ITW framework) to achieve a high propylene/propane separation selectivity partially due to an order of magnitude difference in Henry's constants as shown by gravimetry and Monte Carlo calculations at 353 K.[35,36] A strong effect of molecular size was also noted via thermogravimetry,[7,37,38] ^{13}C NMR,[38] and FTIR[7,37,39] for alkane adsorption on FER, a zeolite containing narrow 8-MR (3.5 Å) and 10-MR (4.2 Å) channels; linear alkanes with a carbon number of 5 or greater adsorb preferentially in the 10-MR channel,[7,38] while branched alkanes adsorb on the exterior of the crystal with the longest alkyl chain either parallel to the surface or protruding into the pore mouth.[37,39]

As anticipated, the trend observed on the other frameworks does not hold for FER as shown in Figure 7; FER is the only zeolite in this study on which adsorption of dihydroxyacetone surpasses that of propylene glycol and therefore adsorption does not consistently increase with an increase in K_{ow}. Similarly, adsorption of C_2-C_6 polyols on FER does not increase with K_{ow}, as shown in Figures S2 and S3 in the Supporting Information, and the systematic increase in adsorption affinity with carbon number noted on MFI, BEA, and ITQ-1 framework materials is also not observed on FER, as shown in our previous work.[12]

Furthermore, a single linear correlation between K_{ads} and K_{ow} is not obtained on FER, as shown in Figure 8. C_3 ketones and 1,ω-diols have an adsorption affinity 1−2 orders of magnitude greater than their branched polyol counterparts (compare dihydroxyacetone/glycerol, hydroxyacetone/propylene glycol, and 1,3-propanediol/propylene glycol); glyceraldehyde adsorption was negligible on this zeolite framework. We postulate that the decrease in K_{ads} with an increase in branching, which is equivalent to an energy difference of 7−11 kJ mol^{-1}, is driven by differences in adsorption configurations. As shown in Figure 8, the ketone correlation on FER is approximately collinear with the correlation found for the 10-MR framework, ITQ-1, indicating that these molecules preferentially adsorb in the 10-MR channel of FER. Since hydroxyacetone and dihydroxyacetone are the only adsorbates in this study that have sp^2 hybridized secondary carbons, it is plausible that their planar molecular configurations allow them to adsorb in the 10-MR channel of FER. It is proposed that branched polyols, like isoalkanes, cannot fully access the 10-MR channel of FER and only adsorb on the external crystal surface resulting in an order of magnitude lower number of adsorption sites[37] as well as a lower heat of adsorption,[7,37] both of which are reflected in the observed decrease in K_{ads}.

dx.doi.org/10.1021/jp208143t |J. Phys. Chem. B 2011, 115, 11431–11438

CONCLUSIONS

A linear correlation between K_{ads} of C_2-C_6 oxygenates on H−ZSM-5 and the readily calculated octanol−water partition coefficient, K_{ow}, was presented, which allows for simple prediction of K_{ads} for these molecules. Decoupling the intrinsic K_{ads} values from the adsorbate infinite dilution activity coefficient in water revealed that, although water−adsorbate interactions in the bulk phase have an effect on zeolite adsorption, an exponential dependence of K_{ads} on adsorbate carbon number is still observed, which indicates that confinement of the adsorbate in the zeolite pore is a critical factor in adsorption. This conclusion is also supported by the observation that there is an increase in K_{ads} with decreasing zeolite pore size for all C_3 adsorbates in this study.

Correlations between K_{ads} and K_{ow} were also identified for the FAU, BEA, and ITQ-1 (MWW) zeolites, indicating the applicability and tunability of the $K_{ads}-K_{ow}$ correlation for a variety of zeolite frameworks. The only exceptions to the correlation were found for bulky 1,2,ω-triols on H−ZSM-5 and all adsorbates on the FER framework, which emphasizes not only the effect of adsorbate functionality on adsorption, but also the role of zeolite topology on adsorption. Overall, these data may be applied to elucidate the interactions responsible for separations of oxygen-containing molecules using zeolite adsorbents.

ASSOCIATED CONTENT

Supporting Information. Molecules used to calculate RMSE values for the K_{ow} calculation methods (Table S1), K_{ow} values for the adsorbates from the XLogP3 and LogKow computational methods (Table S2), adsorption isotherms for select polyol/zeolite systems (Figures S1−S3), and methodology for K_{ads} extraction for C_6 polyfunctional adsorbates.This material is available free of charge via the Internet at http://pubs.acs.org.

AUTHOR INFORMATION

Corresponding Author

*Phone: (612) 626-3981 (A.B.); (612) 626-0920 (M.T.). Fax: (612) 626-7246. E-mail: abhan@umn.edu (A.B.); tsapatsis@umn.edu (M.T.).

ACKNOWLEDGMENT

This material is based upon work supported in part (A.B., M.T., and HPLC instrumentation) by the Catalysis Center for Energy Innovation, an Energy Frontier Research Center funded by the U.S. Department of Energy, Office of Science, Office of Basic Energy Sciences, under Award No. DE-SC0001004. E.E.M. and J.I.S. were supported by the National Science Foundation (CBET 0855863 and 0756641, respectively). Y.G. was supported by the Petroleum Institute of Abu Dhabi through the ADMIRE (Abu Dhabi−Minnesota Institute for Research Excellence) partnership. Kumar Varoon synthesized ITQ-1.

REFERENCES

(1) Smit, B.; Siepmann, J. I. *Science* **1994**, *264*, 1118.
(2) Eder, F.; Lercher, J. A. *Zeolites* **1997**, *18*, 75.
(3) Eder, F.; Stockenhuber, M.; Lercher, J. A. *J. Phys. Chem. B* **1997**, *101*, 5414.
(4) Denayer, J. F.; Souverijns, W.; Jacobs, P. A.; Martens, J. A.; Baron, G. V. *J. Phys. Chem. B* **1998**, *102*, 4588.
(5) Denayer, J. F.; Baron, G. V.; Martens, J. A.; Jacobs, P. A. *J. Phys. Chem. B* **1998**, *102*, 3077.
(6) Savitz, S.; Siperstein, F.; Gorte, R. J.; Myers, A. L. *J. Phys. Chem. B* **1998**, *102*, 6865.
(7) Eder, F.; Lercher, J. A. *J. Phys. Chem. B* **1997**, *101*, 1273.
(8) Denayer, J. F. M.; Ocakoglu, R. A.; Thybaut, J.; Marin, G.; Jacobs, P.; Martens, J.; Baron, G. V. *J. Phys. Chem. B* **2006**, *110*, 8551.
(9) Lee, C. C.; Gorte, R. J.; Farneth, W. E. *J. Phys. Chem. B* **1997**, *101*, 3811.
(10) Ison, A.; Gorte, R. J. *J. Catal.* **1984**, *89*, 150.
(11) Mirth, G.; Lercher, J. A.; Anderson, M. W.; Klinowski, J. *J. Chem. Soc., Faraday Trans.* **1990**, *86*, 3039.
(12) Mallon, E. E.; Bhan, A.; Tsapatsis, M. *J. Phys. Chem. B* **2010**, *114*, 1939.
(13) De Vos, D. E.; Denayer, J.; van Laar, F.; Baron, G. V.; Jacobs, P. A. *Top. Catal.* **2003**, *23*, 191.
(14) Langhendries, G.; De Vos, D. E.; Baron, G. V.; Jacobs, P. A. *J. Catal.* **1999**, *187*, 453.
(15) Ramachandran, C. E.; Du, H. W.; Kim, Y. J.; Kung, M. C.; Snurr, R. Q.; Broadbelt, L. J. *J. Catal.* **2008**, *253*, 148.
(16) Davis, L. *Bioorg. Chem.* **1973**, *2*, 197.
(17) Yaylayan, V. A.; Harty-Marjors, S.; Ismail, A. A. *Carbohydr. Res.* **1999**, *318*, 20.
(18) SRC. Interactive PhysProp Database Demo. http://www.syrres.com/what-we-do/databaseforms.aspx?id=386.
(19) Sangster Research Laboratories. LOGKOW: A databank of evaluated octanol-water partition coefficients. http://logkow.cisti.nrc.ca/logkow/index.jsp.
(20) Cheng, T.; Zhao, Y.; Li, X.; Lin, F.; Xu, Y.; Zhang, X.; Li, Y.; Wang, R.; Lai, L. *J. Chem. Inf. Model.* **2007**, *47*, 2140.
(21) Ghose, A. K.; Viswanadhan, V. N.; Wendoloski, J. J. *J. Phys. Chem. A* **1998**, *102*, 3762.
(22) Nakamoto, H.; Takahashi, H. *Zeolites* **1982**, *2*, 67.
(23) Olson, D. H.; Haag, W. O.; Lago, R. M. *J. Catal.* **1980**, *61*, 390.
(24) Sano, T.; Kasuno, T.; Takeda, K.; Arazaki, S.; Kawakami, Y. In *Progress in Zeolite and Microporous Materials, Parts A−C*; Elsevier Science: Amsterdam, 1997; Vol. 105, p 1771.
(25) Flanigen, E. M.; Bennett, J. M.; Grose, R. W.; Cohen, J. P.; Patton, R. L.; Kirchner, R. M.; Smith, J. V. *Nature* **1978**, *271*, 512.
(26) Krishna, R.; van Baten, J. M. *Langmuir* **2010**, *26*, 10854.
(27) Smit, B.; Maesen, T. L. M. *Nature* **1995**, *374*, 42.
(28) Vlugt, T. J. H.; Zhu, W.; Kapteijn, F.; Moulijn, J. A.; Smit, B.; Krishna, R. *J. Am. Chem. Soc.* **1998**, *120*, 5599.
(29) Ruthven, D. M. *Principles of Adsorption and Adsorption Processes*; John Wiley & Sons, Inc.: New York, 1984.
(30) Suleiman, D.; Eckert, C. A. *J. Chem. Eng. Data* **1994**, *39*, 692.
(31) Nguyen, C. M.; Reyniers, M.-F.; Marin, G. B. *Phys. Chem. Chem. Phys.* **2010**, *12*, 9481.
(32) Tochigi, K.; Uchiyama, M.; Kojima, K. *Korean J. Chem. Eng.* **2000**, *17*, 502.
(33) Chen, B.; Siepmann, J. I. *J. Am. Chem. Soc.* **2000**, *122*, 6464.
(34) June, R. L.; Bell, A. T.; Theodorou, D. N. *J. Phys. Chem.* **1990**, *94*, 1508.
(35) Yang, X. B.; Camblor, M. A.; Lee, Y.; Liu, H. M.; Olson, D. H. *J. Am. Chem. Soc.* **2004**, *126*, 10403.
(36) Olson, D. H.; Yang, X. B.; Camblor, M. A. *J. Phys. Chem. B* **2004**, *108*, 11044.
(37) Pieterse, J. A. Z.; Veefkind-Reyes, S.; Seshan, K.; Lercher, J. A. *J. Phys. Chem. B* **2000**, *104*, 5715.
(38) van Well, W. J. M.; Cottin, X.; de Haan, J. W.; Smit, B.; Nivarthy, G.; Lercher, J. A.; van Hooff, J. H. C.; van Santen, R. A. *J. Phys. Chem. B* **1998**, *102*, 3945.
(39) Yoda, E.; Kondo, J. N.; Wakabayashi, F.; Domen, K. *Phys. Chem. Chem. Phys.* **2003**, *5*, 3306.
(40) Leo, A.; Hoekman, D. *Perspect. Drug Discovery Des.* **2000**, *18*, 19.

(41) Viswanadhan, V. N.; Ghose, A. K.; Revankar, G. R.; Robins, R. K. *J. Chem. Inf. Comput. Sci.* **1989**, *29*, 163.
(42) Meylan, W.; Howard, P. *Perspect. Drug Discovery Des.* **2000**, *19*, 67.
(43) Advanced Chemistry Development Inc. http://www.acdlabs.com.
(44) Moriguchi, I.; Hirono, S.; Liu, Q.; Nakagome, I.; Matsushita, Y. *Chem. Pharm. Bull.* **1992**, *40*, 127.
(45) Tetko, I. V.; Tanchuk, V. Y.; Villa, A. E. P. *J. Chem. Inf. Comput. Sci.* **2001**, *41*, 1407.
(46) Tetko, I. V.; Tanchuk, V. Y. *J. Chem. Inf. Comput. Sci.* **2002**, *42*, 1136.